Bulk and surface states of a doped superlattice

Godfrey Gumbs and Abdulmalik Salman
Department of Physics, University of Lethbridge, Lethbridge, Alberta, Canada T1K 3M4
(Received 12 October 1989; revised manuscript received 2 January 1990)

This paper presents a model calculation of the uncorrelated bulk and surface states of a superlattice, simulated by the Kronig-Penney model, with a periodic array of defects. Inside each quantum well, there is a defect barrier. Explicit results are obtained for the bulk dispersion relation for the minibands for two types of defects: (a) rectangular and (b) triangular. We examine the bulk band structure as a function of the width of the defect and its position within the quantum well. We also calculate the bulk band structure when two defects are inserted inside the well. The virtual surface states for the doped superlattice when an external electric field is applied at the surface are also obtained.

I. INTRODUCTION

Modern techniques such as molecular-beam epitaxy, have made it possible to produce III-V compound semiconductors with well-defined electronic and transport properties. Layered semiconducting superlattices have been used in high-performance optoelectronic devices, for example. Recently, very narrow potential barrier profiles have been produced in $GaAs/Al_xGa_{1-x}As$ superlattices.[1,2] The intentional doping has been implemented by positioning Si donors and Be acceptors in precise numbers during the molecular-beam-epitaxy growth of GaAs layers. This so-called sheet-doping (or δ-doping) technique was originally proposed by Wood *et al.*[3] Since then, it has been applied in advance semiconductor-device concepts. GaAs sawtooth-doping superlattices, consisting of a periodic sequence of alternating *n*- and *p*-type δ-doping layers equally spaced by undoped regions emit light of high intensity.[4] It has been suggested as an application in photonic devices. Also the confinement of donors or acceptors to selectively doped $GaAs/Al_xGa_{1-x}As$ heterostructures leads to high mobilities and to high two-dimensional carrier densities. Therefore, these selectively doped heterostructures might find applications in transistors with improved driving capabilities.

Historically, the Kronig-Penney model[5] has been regarded as an idealized but successful method of calculating the band structure of crystalline solids with periodic potentials. This simple one-dimensional model has mainly been used to study the qualitative nature of bulk crystals. In recent times it has been applied to the study of surface states of crystal structures[6–8] as well as semiconductor superlattices.[9] In the latter case, the discontinuities in the conduction and valence bands for $GaAs/Al_xGa_{1-x}As$ give rise to potential wells for the carriers. The electron effective mass is different in the well and barrier layers of superlattices, in contrast to a constant effective mass in bulk crystalline materials. This difference in the effective mass has been taken into account at the well-barrier interface when applying the Kronig-Penney model to superlattices to obtain the electron wave functions and band energies. This matching procedure has been carried out by Bastard[10,11] who showed that the probability current would be continuous at an interface if the first derivative of the wave function divided by effective mass is continuous. Several other boundary conditions have been proposed for the electron wave function and its derivative.[12,13] However, Bastard's boundary condition is the most intuitive and is straightforward to apply.

A model calculation of the electronic states of a superlattice of period a interleaved with a periodic array of δ-function impurity centers located in the barrier layers has been presented by Beltram and Capasso.[14] In Ref. 14, it was discovered that through a judicious choice of the width of the quantum well and of the location of the impurity within the barrier, the width of the minibands could be controlled. It was shown that when the defects are *centered* in the barriers the energy gap at the Brillouin-zone boundary (π/a) could be closed for certain combinations of the barrier and quantum-well widths. As the distance s of the defect from the center of the barrier increases the gap reopens at π/a. More recently Peeters and Vasilopoulos[15] examined the effects of introducing a rectangular defect of width d into the quantum wells of a superlattice structure. These authors showed that for a certain value of d, the gap at π/a could close when the defect is *centered* inside the well.

Several years ago, Lin and Smit[16] claimed that for certain depths of the potential wells of the Kronig-Penney model (*without defects*), one of the energy gaps at the Brillouin-zone boundary may be zero. They explained this by showing that if both the barrier and quantum well contain an integral number of half waves, the energy gap of the corresponding wave number must be zero. Their numerical results also show that sufficiently deep triangular potential wells can give rise to zero energy gaps.[16] In this paper, we calculate the effects on the bulk band structure when two *rectangular* defect barriers are inserted in the quantum wells of a superlattice. We also study the minibands of a superlattice which contain positive *triangular* defects in the quantum wells. In addition, we

determine the virtual surface states in the presence of an external electric field at the surface of a superlattice containing defects in the quantum wells.

The paper is arranged as follows. In Sec. II the dispersion relation for the energy bands of a bulk superlattice having two rectangular potential barriers per well is obtained. Numerical results are presented for one as well as two defects. The bulk band dispersion relation for a triangular potential profile is calculated. In Sec. III we calculate the virtual surface states for a superlattice with defects.

II. BULK DISPERSION RELATION FOR A SUPERLATTICE WITH DEFECTS

In this section we derive the dispersion relation for the Kronig-Penney model in which two rectangular defects are positioned in each quantum well. The potential profile for the two-defect problem is shown in Fig. 1. The defects are located at distances s_1 and s_2 from the centers of the quantum wells. a is the period and the widths of the defect barriers are d_1 and d_2. The width of the well is w and that of each barrier separating two adjacent wells is b so that $a=b+w$. The electron effective mass is m_w^*, m_b^*, $m_{d_1}^*$, and $m_{d_2}^*$ inside the quantum well, the barrier, and the first and second defect, respectively. The superlattice direction of growth is along the z axis.

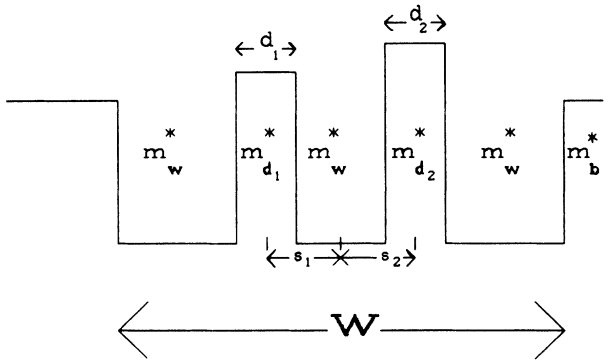

FIG. 1. Barrier representation of the potential field in a superlattice containing two defect barriers of width d_1 and d_2. The centers of the defects are at distances s_1 and s_2 from the middle of the quantum well. The width of the quantum well is equal to w.

If we choose the zero point of energy at the bottom of the quantum well, the potential energy is zero there. We employ the Bastard[10,11] boundary condition at the interfaces and use the Bloch condition as well. After a straightforward mathematical calculation, we obtain the dispersion relation for electrons of energy E and Bloch wave number k_z as

$$\begin{aligned}\cos(k_z a)=&\cosh(k_b b)\{[\cosh(k_1 d_1)\cosh(k_2 d_2)-\eta_{d_1}^-\eta_{d_2}^-\sinh(k_1 d_1)\sinh(k_2 d_2)]\cos k_w(w-d_1-d_2)\\&+[\eta_{d_1}^-\sinh(k_1 d_1)\cosh(k_2 d_2)+\eta_{d_2}^-\cosh(k_1 d_1)\sinh(k_2 d_2)]\sin[k_w(w-d_1-d_2)]\\&+\eta_{d_1}^+\eta_{d_2}^+\sinh(k_1 d_1)\sinh(k_2 d_2)\cos[k_w(w-2s_1-2s_2)]\}\\&+\eta_b^-\sinh(k_b b)\{[\cosh(k_1 d_1)\cosh(k_2 d_2)-\eta_{d_1}^-\eta_{d_2}^-\sinh(k_1 d_1)\sinh(k_2 d_2)]\\&\times\sin[k_w(w-d_1-d_2)]-[\eta_{d_1}^-\sinh(k_1 d_1)\cosh(k_2 d_2)+\eta_{d_2}^-\cosh(k_1 d_l)\\&\times\sinh(k_2 d_2)]\cos[k_w(w-d_1-d_2)]\\&+\eta_{d_1}^+\eta_{d_2}^+\sinh(k_1 d_1)\sinh(k_2 d_2)\sin[k_w(w-2s_1-2s_2)]\}\\&+\eta_b^+\sinh(k_b b)(\eta_{d_2}^+\sinh(k_2 d_2)\{\cosh(k_1 d_1)\cos k_w(d_1-2s_2)]\\&-\eta_{d_1}^-\sinh(k_1 d_1)\sin[k_w(d_1-2s_2)]\}\\&+\eta_{d_1}^+\sinh(k_1 d_1)\{\cosh(k_2 d_2)\cos[k_w(d_2-2s_1)]-\eta_{d_2}^-\sinh(k_2 d_2)\\&\times\sin[k_w(d_2-2s_1)]\}\})\ . \end{aligned}\tag{1}$$

The electron wave number in the well is $k_w\equiv(2m_w^*E/\hbar^2)^{1/2}$. The wave numbers in the barriers and in the defects are given by

$$k_b\equiv\frac{\sqrt{2m_b^*(V_b-E)}}{\hbar},\quad k_i\equiv\frac{\sqrt{2m_{d_i}^*(V_{d_i}-E)}}{\hbar}\ ,\tag{2}$$

respectively, where V_b is the potential energy of the barrier and V_{d_i} is the potential energy of an electron in a defect ($i=1,2$). In this notation we have introduced the following quantities:

$$\eta_b^{\pm}=\frac{\lambda_b^2k_b^2\pm k_w^2}{2\lambda_b k_b k_w},\quad \eta_{d_i}^{\pm}=\frac{\lambda_{d_i}^2k_i^2\pm k_w^2}{2\lambda_{d_i}k_i k_w}\ ,\tag{3}$$

where $\lambda_b=m_w^*/m_b^*$ and $\lambda_{d_i}=m_w^*/m_{d_i}^*$. The result for a single defect within each period is easily obtained by setting $d_1=0$, for example, in Eq. (1) while keeping d_2 finite. The derived formula agrees with the result of Peeters and Vasilopoulos.[15]

We have carried out numerical calculations for the miniband energies using Eq. (1). In these calculations we

assume that the quantum wells are made out of GaAs and the barriers and defects out of the material $Al_xGa_{1-x}As$, where x is different for the barrier and the defect. Of course, different types of material could be used for the defect barriers. The electron effective mass in the alloy $Al_xGa_{1-x}As$ is given by $m^*/m_e = 0.067+0.083x$ and the barrier height is taken to be $V_0=(0.693x+0.222x^2)$ eV. The key result of Ref. 15 is that the band gaps at the Brillouin-zone boundary could be closed by adjusting the width of the defect when it is located in the *middle* of the well. When the defect is displaced from this position, the gap at the Brillouin-zone boundary is always finite. This curious result has motivated us to carry out the present calculation involving two defects per period. In Fig. 2, we set $d_1=0$ in Eq. (1) and calculate the lower and upper bounds of the two lowest minibands as a function of the position of the second defect barrier from the center of the well. Our numerical calculations show that the band gaps at the Brillouin-zone boundary increase as a function of the distance s_2 of the defect from the center of the well. Only when $s_2=0$ were we able to obtain a value of d_2 for which the gap energy is equal to zero. Figure 3 shows a plot of the first two minibands of a superstructure having two defects in each of the quantum wells as a function of the width of one of these defects at a distance s_2 from the center of the well while the one having width d_1 is located at a distance s_1 from the center of the well. Consistent with the results of our numerical calculations for a superlattice having a single defect in each quantum well, we find that because one of the two defects is displaced from the middle of the well, the energy gap at the Brillouin zone is finite for all values of defect width and heights of the defect potential barrier.

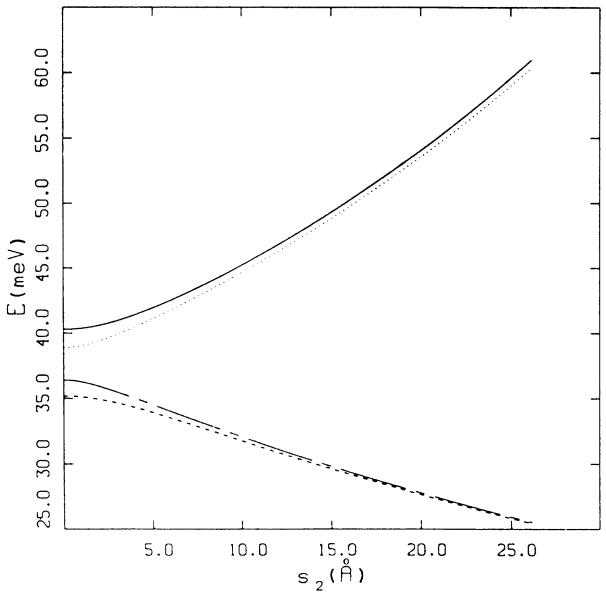

FIG. 2. Calculated energies of the first two minibands as a function of the distance s_2 of a rectangular defect from the center of the potential well. The results are based on Eq. (1) with $d_1=0$ and $d_2=25$ Å, i.e., we assume that only one defect is present in each period. The barrier width $b=50$ Å and the width of the well is taken to be $w=200$ Å. We take $x=0.3$ for the $Al_xGa_{1-x}As$ in the barrier and $x=0.4$ for the defect.

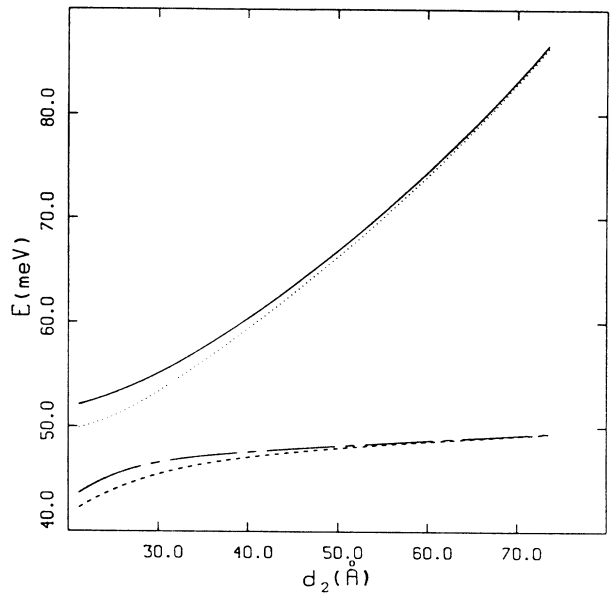

FIG. 3. The lower and upper bounds of the first two minibands of a superlattice having two defects in each quantum well (see Fig. 1). The defects have widths d_1 and d_2 and are located at $s_1=25$ Å and $s_2=25$ Å, respectively. We choose $d_1=20$ Å and assume that both defects as well as the barriers separating the wells are made of $Al_xGa_{1-x}As$. We take $x=0.2$ for both the barrier and the defects.

III. SUPERLATTICE WITH TRIANGULAR DEFECTS

In this section we compliment our calculations of the band structure for the Kronig-Penney model containing defects inside the quantum well for which the potential profile is rectangular to a model in which the defect potentials are triangular (see Fig. 4). Following the procedure outlined in Ref. 17, for an isolated triangular barrier, we apply the Bastard[10,11] boundary condition to calculate the band structure for the structure schematically represented in Fig. 4. The general solution of the Schrödinger equation in the wedge-shaped region is a linear combination of Airy functions Ai(x) and Bi(x).[18]

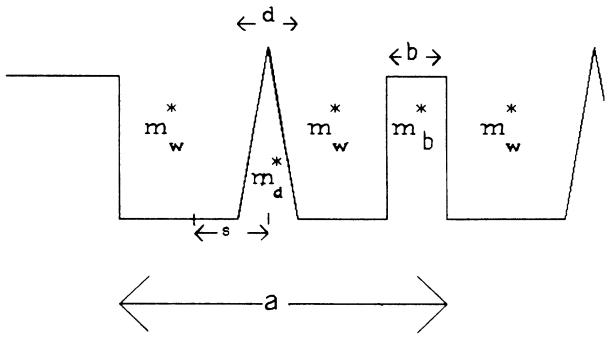

FIG. 4. Square-well periodic potential (Kronig-Penney model), with triangular defects.

Let w be the width of the quantum well, b the width of the quantum well, b the width of the barrier, and d the basal width of the triangular defect. We take s to be the displacement of the center of the triangular barrier from the middle of the well.

We introduce notation by writing down the solutions of the Schrödinger equation in the various regions of Fig. 4. We have

$$\psi_{w;1}(z)=A\exp(ik_w z)+B\exp(-ik_w z),\quad 0\le z\le \xi_1\ ; \tag{4a}$$

$$\psi_{d;1}(z)=C\,\mathrm{Ai}(\zeta)+D\,\mathrm{Bi}(\zeta),\quad \xi_1\le z\le \frac{w}{2}+s\ ; \tag{4b}$$

$$\psi_{d;2}(z)=E\,\mathrm{Ai}(\eta)+F\,\mathrm{Bi}(\eta),\quad \frac{w}{2}+s\le z\le \xi_2\ ; \tag{4c}$$

$$\psi_{w;2}(z)=G\exp(ik_w z)+H\exp(-ik_w z),\quad \xi_2\le z\le w\ , \tag{4d}$$

$$\psi_b(z)=J\exp(-k_b z)+K\exp(k_b z),\quad w\le z\le a\ ; \tag{4e}$$

where $\xi_{1,2}\equiv(w+2s\mp d)/2$. We have introduced the following change of variables:

$$\zeta\equiv\left[\frac{d}{2\kappa_0^2}\right]^{2/3}\left[\kappa_0^2-k_w^2+\frac{2x}{d}\kappa_0^2\right],$$

$$\eta\equiv\left[\frac{d}{2\kappa_0^2}\right]^{2/3}\left[\kappa_0^2-k_w^2-\frac{2x}{d}\kappa_0^2\right], \tag{5}$$

where $x\equiv z-(w/2+s)$. We have also introduced the wave number κ_0 defined by $\kappa_0\equiv\sqrt{2m_d^* V_0/\hbar^2}$ where V_0 is the height of the defect at the apex of the triangle. Matching $\psi(z)$ and $m^{*-1}d\psi(z)/dz$ for the wave functions, given in Eqs. (4), within a period of the superlattice we obtain the transfer matrices relating the constant coefficients appearing in the wave functions. Applying this in conjunction with the Bloch condition we obtain the eigenvalue equation for the electronic state with wave number k_z and energy E. It is given by

$$\begin{bmatrix}A\\B\end{bmatrix}=\mathbf{M}_5\mathbf{M}_4\mathbf{M}_3\mathbf{M}_2\mathbf{M}_1 e^{ik_z a}\begin{bmatrix}A\\B\end{bmatrix}, \tag{6}$$

where the transfer matrices are

$$\mathbf{M}_1=\pi\begin{bmatrix} e^{ik_w\xi_1}t_d^-(\zeta_1) & e^{-ik_w\xi_1}t_d^+(\zeta_1)\\ -e^{ik_w\xi_1}S_d^-(\zeta_1) & -e^{-ik_w\xi_1}S_d^+(\zeta_1)\end{bmatrix} \tag{7a}$$

$$\mathbf{M}_2=\pi\begin{bmatrix}\mathrm{Ai}(\mu)\mathrm{Bi}'(\mu)+\mathrm{Ai}'(\mu)\mathrm{Bi}(\mu) & 2\,\mathrm{Bi}(\mu)\mathrm{Bi}'(\mu)\\ -2\,\mathrm{Ai}(\mu)\mathrm{Ai}'(\mu) & -[\mathrm{Ai}(\mu)\mathrm{Bi}'(\mu)+\mathrm{Ai}'(\mu)\mathrm{Bi}(\mu)]\end{bmatrix} \tag{7b}$$

$$\mathbf{M}_3=\frac{1}{2}\begin{bmatrix}[\mathrm{Ai}(\zeta_1)-r_d\mathrm{Ai}'(\zeta_1)]e^{-ik_w\xi_2} & [\mathrm{Bi}(\zeta_1)-r_d\mathrm{Bi}'(\zeta_1)]e^{-ik_w\xi_2}\\ [\mathrm{Ai}(\zeta_1)+r_d\mathrm{Ai}'(\zeta_1)]e^{-ik_w\xi_2} & [\mathrm{Bi}(\zeta_1)+r_d\mathrm{Bi}'(\zeta_1)]e^{-ik_w\xi_2}\end{bmatrix} \tag{7c}$$

$$\mathbf{M}_4=\frac{1}{2}\begin{bmatrix}T_b^- e^{(k_b+ik_w)w} & T_b^+ e^{(k_b-ik_w)w}\\ T_b^+ e^{-(k_b-ik_w)w} & T_b^- e^{-(k_b+ik_w)w}\end{bmatrix} \tag{7d}$$

$$\mathbf{M}_5=\frac{1}{2}\begin{bmatrix}R_b^- e^{-k_b a} & R_b^+ e^{k_b a}\\ R_b^+ e^{-k_b a} & R_b^- e^{k_b a}\end{bmatrix}. \tag{7e}$$

Here $\zeta_1\equiv-(dk_0^3/2\kappa_0^2)^{2/3}$ and $\mu\equiv(d\kappa_0/2)^{2/3}(1-k_0^2/\kappa_0^2)$,

$$t_d^{\pm}(\zeta_1)\equiv\mathrm{Bi}'(\zeta_1)\pm\frac{\mathrm{Bi}(\zeta_1)}{r_d}\ ,$$

$$S_d^{\pm}(\zeta_1)\equiv\mathrm{Ai}'(\zeta_1)\pm\frac{\mathrm{Ai}(\zeta_1)}{r_d}\ , \tag{8}$$

with $r_d\equiv-i\lambda_d/\sqrt{-\zeta_1}$, where λ_d has been defined in Sec. II. We have also introduced the quantities

$$T_b^{\pm}\equiv 1\pm\frac{1}{R_b},\quad R_b^{\pm}\equiv 1\pm R_b\ , \tag{9}$$

where $R_b\equiv-i\lambda_b k_b/k_w$. The determinant of the product of the matrices in Eq. (6) is equal to unity. Therefore, the dispersion relation for wave number k_z and energy E is given by

$$\cos(k_z a)=\tfrac{1}{2}\mathrm{Tr}[\mathbf{M}_5\mathbf{M}_4\mathbf{M}_3\mathbf{M}_2\mathbf{M}_1]\ , \tag{10}$$

where Tr [$\cdots$] means that the trace of a matrix is to be taken. We have carried out numerical calculations for the dispersion relation in Eq. (10) making use of Eqs. (7) for the transfer matrices. In Fig. 5 we plot the calculated energies for the first two minibands as a function of the *basal* width d of triangular defects centered in the middle of the quantum wells. This demonstrates that the separation between the minibands decreases as the defect width increases up to $d=30$ Å and remains closed up to $d=35$ Å. When the defects have their centers displaced from the middle of the wells, this range of defect widths for which the gap remains closed decreases until $s\approx 10$ Å. This is, of course, in contrast to the superlattice with rec-

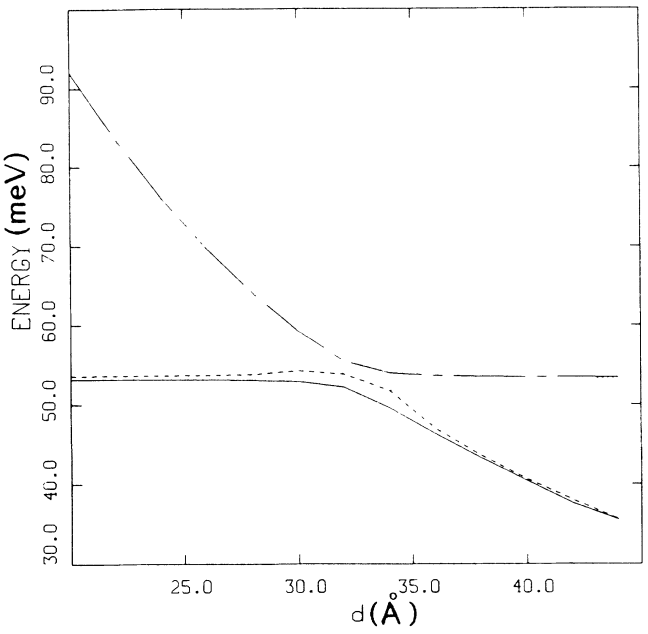

FIG. 5. This figure shows the two lowest minibands as a function of the basal width of triangular defects located in the middle of quantum wells. We assume that the defects and barriers are made from the alloy $Al_xGa_{1-x}As$ and take $x=0.3$ for the barrier and $x=0.4$ for the defects. The barrier width $b=50$ Å and the width of each well is taken to be $w=200$ Å.

tangular defects which we discussed in Sec. II. We have also carried out calculations when the triangular defects are asymmetric about the perpendicular line drawn from the apex to the base. Our numerical calculations show that in this case the defects could have their centers displaced from the middle of the wells and we could have the miniband separation at the Brillouin-zone boundary vanishing for a range of values of the displacement s.

IV. VIRTUAL SURFACE STATES FOR A DOPED SUPERLATTICE WITH DEFECTS

The results presented so far have been concerned with calculations of the energy bands of doped superlattices in bulk. We now turn our attention to the effects generated by an applied electric field on the properties of surface states in semiinfinite superlattices which contain positive defects in the walls. We restrict our attention to the case when the potential field produced by the defects is rectangular. This problem is of some interest since there has been a considerable amount of work on the properties of *virtual* surface states, i.e., surface states in the presence of a negative electric field, and the associated electron tunneling from these states through the linear potential barrier.[6,7] We assume that the semi-infinite superlattice occupies the negative half-space ($z\leq 0$) with vacuum in the positive half-space. The potential in the vacuum region has a constant value V_0 for time $t<0$, before it changes suddenly at $t=0$ to the linear potential $V(z)=V_0-\gamma z$ for $t>0$. There is a screen located at $z=D$ which is represented by an infinitely high potential barrier (Fig. 6).

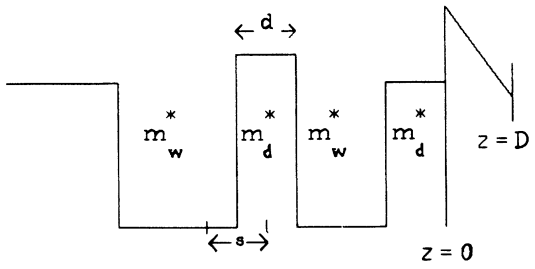

FIG. 6. Potential profile for a doped semi-infinite semiconductor superlattice with an applied electric field γ. For time $t<0$, the potential in the vacuum region is constant and equal to V_0. For $t>0$ the potential is $V(z)=V_0-\gamma z$. The screen located at $z=D$ is represented by an infinitely high potential barrier.

The wave function in the linear potential region $0<z<D$ is the Airy function solution

$$\psi_{II}(z)=C_1\mathrm{Ai}(u)+C_2\mathrm{Bi}(u)\ , \tag{11}$$

where

$$u=(2m_0/\hbar^2\gamma^2)^{1/3}(V_0-\gamma z-E)\ , \tag{12}$$

where m_0 is the free-electron mass. The solution of the Schrödinger equation in the barrier region between $z=0$ and $z=-b$ is given by

$$\psi_b(z)=J\exp(-k_bz)+K\exp(k_bz),\quad -b\leq z\leq 0\ . \tag{13}$$

The wave function vanishes at $z=D$ [i.e., $\psi_{II}(D)=0$]. Using this in conjunction with the continuity of the wave function and $m^{*-1}d\psi(z)/dz$ at $z=0$, we obtain after a little algebra

$$(k_b-\Omega)J=(k_b+\Omega)K\ , \tag{14}$$

where

$$\Omega=\frac{m_b^*}{m_0}\left[\frac{2\gamma m_0}{\hbar^2}\right]^{1/3}\frac{\mathrm{Ai}(u_1)\mathrm{Bi}'(u_0)-\mathrm{Ai}'(u_0)\mathrm{Bi}(u_1)}{\mathrm{Ai}(u_1)\mathrm{Bi}(u_0)-\mathrm{Ai}(u_0)\mathrm{Bi}(u_1)}\ , \tag{15}$$

with $u_0\equiv u(z=0)$ and $u_1\equiv u(z=D)$. The eigenfunctions in the various regions of the superlattice within a period a can be written down in a straightforward way. Our calculations show that the eigenvalue equation for the electronic state with wave number k_z and energy E is given by

$$\begin{bmatrix}J\\K\end{bmatrix}=\mathbf{Q}e^{ik_za}\begin{bmatrix}J\\K\end{bmatrix}\ , \tag{16}$$

where $\mathbf{Q}$ is a product of 2×2 transfer matrices relating the coefficients of the electronic wave functions of the superlattice. From Eqs. (14) and (15) we obtain the dispersion relation for virtual surface states:

$$\cos(k_z a)=\frac{1}{2}\frac{1+\left[Q_{11}+Q_{12}\left[\frac{k_b-\Omega}{k_b+\Omega}\right]\right]^2}{Q_{11}+Q_{12}\left[\frac{k_b-\Omega}{k_b+\Omega}\right]} \tag{17}$$

where Q_{11} and Q_{12} are the elements in the first row of the 2×2 matrix $\mathbf{Q}$. When there are double rectangular defects in each quantum well, $\cos(k_z a)$ is given by Eq. (1). In the limit when there is just one rectangular defect per quantum well, we have

$$\begin{aligned}Q_{11}=e^{-k_b b}\{&\cosh(k_d d)\cos[k_w(w-d)]-\eta_b^-\cosh(k_d d)\sin[k_w(w-d)]\\&-\eta_d^-\sinh(k_d d)\sin[k_w(w-d)]\\&-\eta_b^+\eta_d^+\sinh(k_d d)\cos(2k_w s)+\eta_b^-\eta_d^-\sinh(k_d d)\cos[k_w(w-d)]\}\end{aligned} \tag{18}$$

and

$$\begin{aligned}Q_{12}=e^{-k_b b}\{&\eta_b^+\cosh(k_d d)\sin[k_w(w-d)]-\eta_d^+\sinh(k_d d)\sin(2k_w s)\\&-\eta_b^+\eta_d^-\sinh(k_d d)\cos[k_w(w-d)]+\eta_b^-\eta_d^+\sinh(k_d d)\cos(2k_w s)\}\end{aligned} \tag{19}$$

Here d is the width of the defects and s is the distance of the center of each defect from the middle of the wells. We can now substitute these results for Q_{11} and Q_{12} into the surface dispersion relation in Eq. (17).

We have calculated surface states using Eqs. (17)–(19). In Fig. 7 we plot the surface energies as a function of the width d of rectangular defects centered in the middle of the wells. We show plots when an electric field is applied and also when the electric field is zero. We chose the electric field $\gamma=0.5$ eV/Å and, for both Figs. 7(a) and 7(b), we take the constant potential in the vacuum region $V_0=0.4$ eV, the distance $D=2$ cm. The widths of the well and the defect are $w=200$ Å and $d=20$ Å, respectively. Here we see that there are two surface states for the superstructure. When an electric field is applied the surface states get closer to each other as the width d of the defect increases up to $d=18$ Å and then they separate with increasing values of d. When the electric field $\gamma=0$, our calculations show that the surface states move closer to each other with increasing defect width up

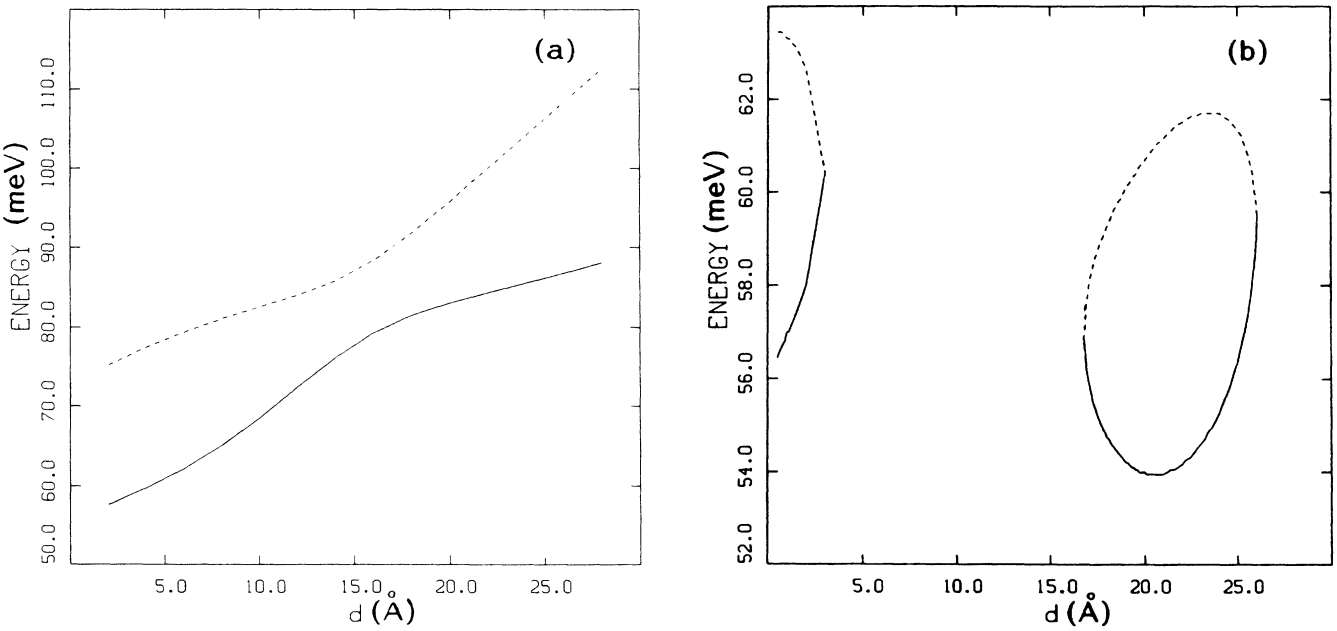

FIG. 7. Energy of surface states as a function of the width d of defects centered in the middle of the wells. In (a) an electric field $\gamma=0.5$ eV/Å is applied at time $t>0$ in the vacuum region $z>0$. In (b) there is no applied electric field. The parameters chosen for the constant potential V_0, the width d of the defect, and w for the quantum well are given in the text. The concentration x of Al in the defect and the barrier, both of which are chosen to be $Al_xGa_{1-x}As$, is also given in the text.

to $d=3$ Å, where there is just one surface state. As the width of the defect barrier increases, we find that there is a range of values of d for which there are no surface states. For 17 Å $\leq d \leq 25$ Å we find two surface states. For $d>25$ Å, there are no surface states. Of course, these results have interesting implications for the field emission of electrons from surface states.[6]

V. CONCLUDING REMARKS AND SUMMARY

In this paper we have presented a calculation for the minibands of a superlattice which has positive defects in the quantum wells of the superlattice. The bulk dispersion relation has been calculated analytically when there are two *rectangular* defects present within the quantum wells. We have also calculated the transfer matrices for a structure having one triangular defect in each quantum well. Numerical results for the minibands have been obtained as a function of the width of the defects as well as the displacement s of the center of the defect from the middle of the wells. When there is a periodic repetition of only one *rectangular* defect in every quantum well, we have found that the minigaps of the superlattice at the Brillouin-zone boundary do not close when the distance s is finite. Only when $s=0$, could the minigaps close for a certain width (or height) of the defects.[15] As a matter of fact, in the nearly-free-electron approximation, the band gap on the Bragg plane is equal to twice the magnitude of the Fourier component $2|V_g|$ of the periodic potential, where $g=2\pi/a$. When there is just one defect in each quantum well, we have

$$|V_g|=\frac{2}{g}\left\{\left[V_d\cos(gs)\sin\left[\frac{gd}{2}\right]-V_b\sin\left[\frac{gb}{2}\right]\right]^2+V_d^2\sin^2(gs)\sin^2\left[\frac{gd}{2}\right]\right\}^{1/2}. \tag{20}$$

Only when $s=0$, could we have $V_g=0$ which corresponds to V_d/V_b equal to $\sin(\pi b/a)/\sin(\pi d/a)$. The agreement between the numerical results obtained from Eq. (1) and the approximate value for the defect width and potential barrier when the band gap at the zone boundary closes is fairly good (10–15%). This could be interpreted as follows. When the wave number k_z is on a Bragg plane, the energy levels (to leading order in the Fourier component V_g), are indistinguishable from their free-electron values for some value of defect width when $s=0$.. This of course, is not possible when the defects are off-centered since the symmetry and/or antisymmetry of the eigenfunctions, with respect to the middle of the quantum wells, is broken. For *two* rectangular defects in each quantum well of the superlattice, our numerical calculations show that the miniband gaps get larger as the distance of the center of the defects from the middle of the wells increases; the gaps do not close when there are *two* rectangular defects in the quantum wells. For triangular defects, we have found novel results for the miniband gaps as a function of the width d of the defects and the distance s of the center of the defects from the middle of the quantum wells. We have found that for $s=0$ the minigaps get narrower as d increases and the gap remains closed for a range of values of d, then the minibands separate again for larger values of d. As s increases the range of values of defect width for which the minigaps remain closed gets smaller until, for sufficiently large values of s, the gap does not close.

The surface states calculated here also show an interesting dependence on the widths of the defect barriers introduced into the quantum wells. In the sudden approximation of time-dependent perturbation theory,[19] we found that when an electric field γ is applied the two surface states get closer together as the width d of the defect increases and then they separate for larger values of d. When $\gamma=0$ our calculations show that there are surface states only for a certain range of values of the defect width d. This, of course, means that the surface-state current could be controlled by varying the width of the defect. Similar results could also be obtained by varying the height of the defects. The integrated density of states for a doped superlattice and the surface-state tunneling will be presented elsewhere.

Several years ago, Glasser[20] presented a general formulation for the thermodynamic potential of an electron gas in the presence of an external magnetic field and a neutralizing electrostatic potential which is periodic along the direction of the magnetic field. In Ref. 20, the thermodynamic potential, from which all equilibrium properties could be calculated, was expressed in terms of the one-dimensional band structure of the solid. We plan to extend Glasser's formulation to a superlattice where the electron effective mass is not uniform along the superlattice growth direction.

ACKNOWLEDGMENTS

This work was supported in part by the Natural Sciences and Engineering Research Council (NSERC) of Canada (G. G.).

[1]K. Ploog, J. Cryst. Growth **81**, 304 (1987).
[2]H. P. Hjalmarson, J. Vac. Sci. Technol. **21**, 524 (1982); Superlatt. Microstruct. **1**, 379 (1985).
[3]C. E. C. Wood, G. Metze, J. Berry, and L. F. Eastman, J. Appl. Phys. **51**, 383 (1980).
[4]K. Ploog, M. Hauser, and A. Fischer, Appl. Phys. A **45**, 233 (1988).
[5]R. L. Kronig and W. G. Penney, Proc. R. Soc. London Ser. A **130**, 499 (1931).
[6]S. G. Davison and M. Kolar, J. Phys. C **18**, 4581 (1985).
[7]M. Steslicka and Z. Perkal, Solid State Commun. **35**, 349 (1980).
[8]M. Steslicka, Prog. Surf. Sci. **5**, 157 (1974).
[9]H.-S. Cho and R. Prucnal, Phys. Rev. B **36**, 3237 (1987).
[10]G. Bastard, Phys. Rev. B **24**, 5693 (1981).
[11]G. Bastard, Phys. Rev. B **25**, 7584 (1982).

[12]Q. Zhu and H. Kroemer, Phys. Rev. B **27**, 3519 (1983).
[13]T. Ando and S. Mori, Surf. Sci. **113**, 124 (1982).
[14]F. Beltram and F. Capasso, Phys. Rev. B **38**, 3580 (1988).
[15]F. M. Peeters and P. Vasilopoulos, Appl. Phys. Lett. **55**, 1106 (1989).
[16]S.- T. Lin and J. Smith, Am. J. Phys. **48**, 193 (1980).
[17]D. ter Haar, *Selected Problems in Quantum Mechanics* (Infosearch, London, 1964), p. 12.
[18]*Handbook of Mathematical Functions,* edited by M. Abramowitz and I. A. Stegun (Dover, New York, 1972).
[19]L. I. Schiff, *Quantum Mechanics* (McGraw-Hill, New York, 1968), p. 292.
[20]M. L. Glasser, J. Phys. Chem. Solids **27**, 1459 (1966).